Symmetries in exfoliated 2D quantum materials

Instructions for the Advanced Lab Course

Supervisors: Katharina Nisi, Ana Mićević

E-Mail: Katharina.nisi@wsi.tum.de // Ana.micevic@wsi.tum.de

Zentrum für Nanotechnologie und Nanomaterialien (ZNN), TUM

Am Coulombwall 4a

85748 Garching

Please read the following theory and instructions very carefully. If you have any questions, ask your advisors on the day of your experiment or before *via* e-mail.

The advanced lab course *symmetries in exfoliated 2D quantum materials* gives insight into the fundamental properties of quantum two-dimensional (2D) materials determined by optical means such as Raman, photoluminescence (PL) and second harmonic generation (SHG) measurements. The aim is an application-orientated understanding of the basic physical phenomena behind Raman and PL signals, as well as SHG measurements. Furthermore, the goal is to learn how to evaluate data and how to extract as manifold information as possible. The questions in the *Theory* chapter are not obligatory to answer but serve as an orientation for your own understanding.

Chandrasekhara Venkata Raman first described the **Raman** effect in 1922. It is based on inelastic scattering of light from a material/sample due to vibrational movement. This light-matter interaction causes an energy shift specific for each material, resulting in unique Raman spectra. Raman spectroscopy is a fast and versatile characterization method that is very sensitive to changes in the electronic structure and therefore often used to investigate 2D materials. It gives insight into vibrational states of molecules or materials. Raman measurements on 2D materials are highly sensitive to symmetry, number of layers, defects as well as strain and doping.[1,2,3]

The lowest order nonlinear optical process is a three-wave mixing process. **Second harmonic generation** ("frequency doubling") is a nonlinear optical process in which two photons of the same frequency are 'combined' through interaction with a nonlinear medium to form a new photon with doubled initial frequency. This effect was first demonstrated in 1961 by *Franken et. al*.[4] SHG is *e.g.* used in laser industry to make green (532 nm) laser light from a 1064 nm source. Furthermore, it is applied in ultra-short pulse measurements and SHG microscopy. SHG can be used for determining the crystal lattice orientation, detect edge states of TMDCs as well as imaging grains and boundaries.

1. Theory

1.1. Raman scattering

For this advanced lab course, a laser wavelength of 532 nm is used for excitation. Most of the laser light passes the sample without any energetic light-matter interaction, but a small part of the light is scattered inelastically, which is referred to as *Raman* scattering (Figure 1). There are two types of Raman scattering: **Stokes** and **Anti-Stokes** scattering: Stokes scattering describes the transfer of energy from the photon to the material, in which case the emitted photon has a lower energy than then absorbed photon (v_0-v_t). Anti-Stokes scattering describes the energy transfer from the material onto the photon, leading to a higher energy of the emitted photon (v_0+v_t). A larger part of the light is scattered elastically, namely the **Rayleigh** (v_0) scattering, which leads to a signal with an unchanged frequency. Raman spectra are usually illustrated as intensity *vs.* Raman shift. The Raman shift is typically reported in relative wavenumbers

$$\Delta v\ [cm^{-1}] = \frac{1}{\lambda_0[nm]} - \frac{1}{\lambda_t[nm]},\tag{1}$$

where λ_0 is the laser wavelength and λ_t is the Raman spectrum wavelength and is directly related to the energy. In contrast, Rayleigh scattering leads to a signal with a Raman shift of zero.
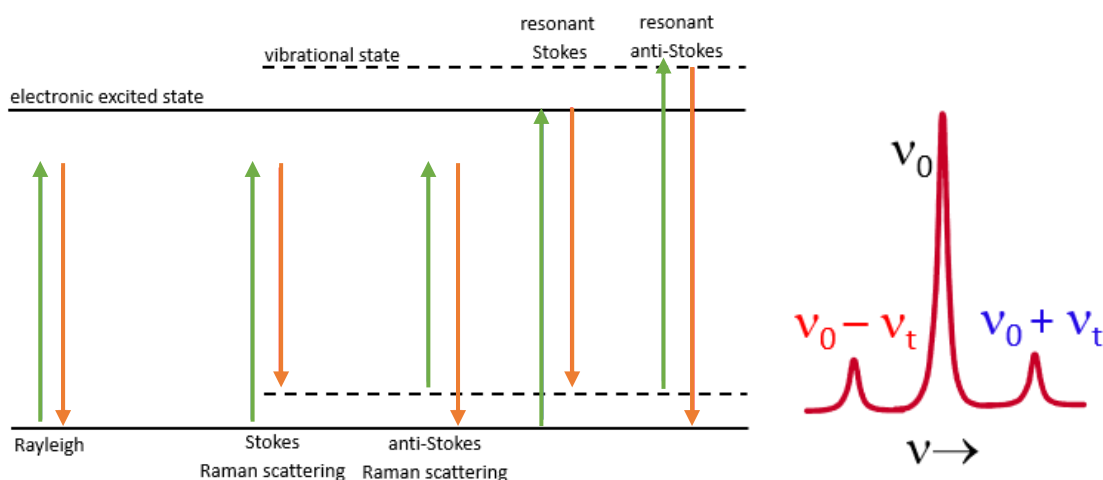

Figure 1: Principles of Raman spectroscopy – Jablonski diagram. Stokes scattering correlates to an energy decrease, Anti-Stokes scattering correlates to an energy increase.

In general, the primary selection rule for Raman active modes is an *anisotropic polarizability* of the molecule. The polarizability α, describes how easy an electric field can distort the electron cloud in an atom or molecule and it is defined as the ratio of the induced dipole moment P, of an atom to the electric field E, that produces the dipole moment

$$P = \alpha E. \tag{2}$$

A few generalities are further helpful:

a) Symmetric vibrations lead to strong Raman signals; asymmetric vibrations lead to weaker Raman signals.

b) Bending vibrational modes lead to weaker Raman signals.

1.1.1. Raman scattering on graphene

To understand the Raman spectra of graphene, the phonon dispersion of graphene must first be understood. The unit cell of monolayer graphene contains two carbon atoms, A and B. Hence, there are six phonon dispersion bands (three acoustic branches (A) and three optic phonon branches (O)). The atomic vibrations are perpendicular to the graphene plane for one optic and one acoustic branch (out-of-plane modes (o)). The vibrations for the other four modes are in-plane (i). Furthermore, the phonon modes are classified as transverse (T; perpendicular) or longitudinal (L; parallel) with respect to the direction of the nearest carbon-carbon atoms.[5]
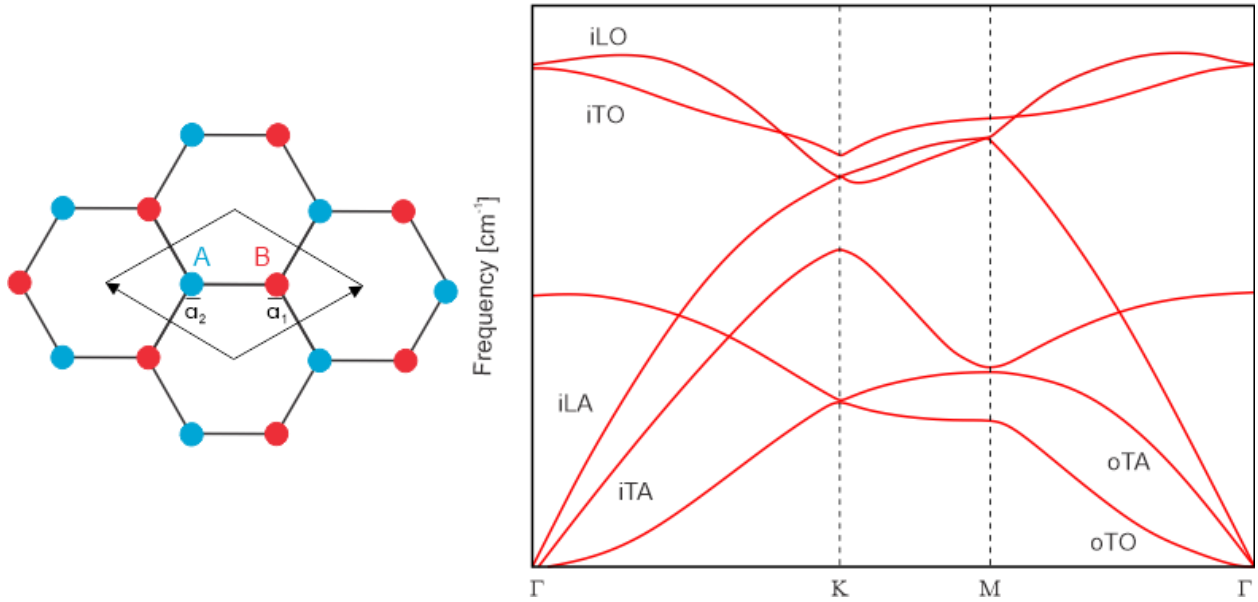

Figure 2: Top view of the real space unit cell of monolayer graphene. The unit cell contains the two inequivalent atoms A and B. Further, the calculated phonon dispersion relation of graphene is shown in reciprocal space (adapted from [5]). The high symmetry points of the Brillouin zone are labelled as K, M and Γ.

The most prominent resonances of graphene in a typical Raman spectrum are the G band (~ 1580 cm⁻¹) and the 2D band (~ 2700 cm⁻¹). The disorder induced D band, breathing mode, (~ 1350 cm⁻¹) is visible in the case of a disordered sample or at the edge of a graphene sample.[5] The G band, a first order Raman scattering process, is associated with the doubly degenerate (iTO and LO) phonon mode (E_{2g} symmetry) at the Brillouin zone center at ~1570 cm⁻¹. The D and 2D bands involve two iTO phonons near the *K*-point for the 2D band or one iTO phonon including defect for the D band. Since the D band is only active in defected graphene, it is an indication of the quality of your sample.[5] Although defect engineering is a field of growing importance, defects are usually unwanted in most applications. Hence, one can quantitatively investigate the defectiveness of graphene samples by calculating the intensity ratio between D mode and G mode (I_D/I_G).[5,6]

Layer number-dependence:

Raman measurements are often utilized to determine the number of layers of many different 2D materials. There are a few key points that can help determine the layer numbers from the typical Raman modes of graphene (G and 2D mode). It has been demonstrated that the intensity of the G peak (linearly) increases and the resonance red shifts with increasing layers. The 2D resonance undergoes a change of the resonance shape in which monolayer graphene exhibits a single Lorentzian function, whereas bilayer graphene splits into multiple Lorentzian components. This can be explained by the double-resonant Raman model: an electron is vertically excited from point A in the π band to point B in the π* band by absorbing a photon.[5] The excited electron is inelastically scattered to a point C by emitting a phonon (wave vector *q*). It is inelastically backscattered to the vicinity of point A by emitting another phonon (wave vector *q*). Lastly, the electron and hole recombine and emit a photon with a smaller energy than the incident photon. For the case of double layer graphene, the π and π* bands split into two bands each, which equals four bands in total and therefore also four different excitations are possible, wherefore the 2D resonance contains four Lorentzian terms.[5,6]
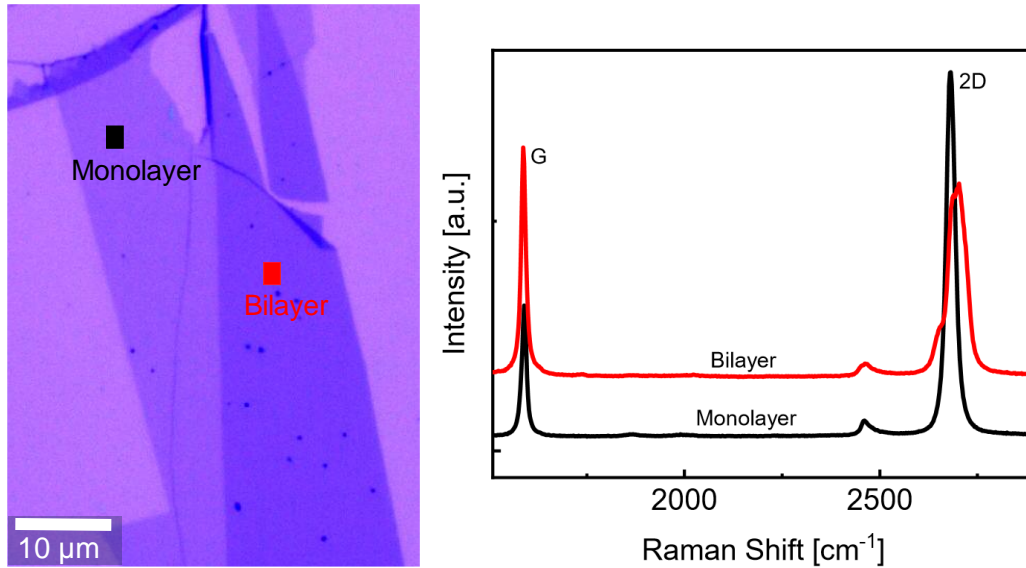
Figure 3:Image of mono- and bilayer graphene (left). Typical spectrum of mono- and bilayer graphene with the G and 2D mode (corresponding to the flakes on the left). 532 nm excitation laser. This figure demonstrates an increase of the G peak and a red shift of the 2D peak for the bilayer as compared to the monolayer graphene.

Following questions are guidelines for you to proof your understanding of Raman spectroscopy:

1. *Include sketches of the breathing and the shear mode.*

2. *Explain the first- and second-order Raman scattering process using following images. Assign and explain the three typical Raman modes to the images using the phonon dispersion relation of Fig 2.*
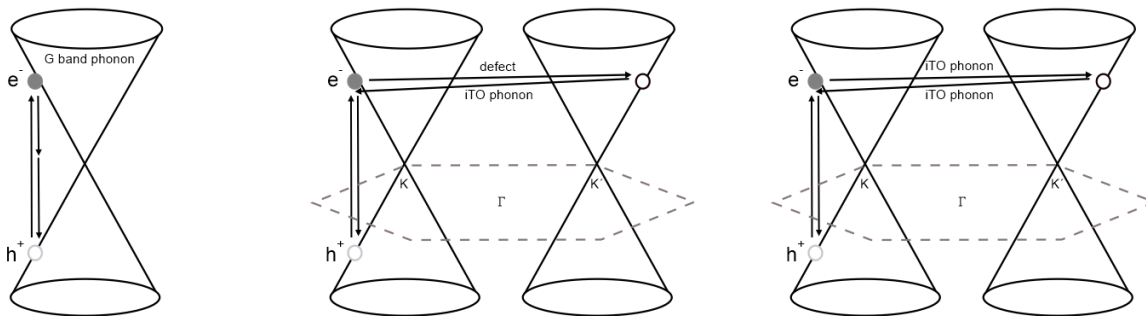
3. *Why is the 2D mode active in pristine graphene but the D mode is not?*

4. *How does the incoming laser power influence a Raman spectrum of graphene? (Which peak is impacted and how?)*

5. *Why is it important to note down the temperature and humidity on the experiment day?*

1.2. Photoluminescence of WS_2

Transition metal dichalcogenides (TMDCs) have gained interest in the field of 2D nanomaterials due to their unique physical and chemical properties. In the single atomic layer limit, TMDCs show strong spin-valley coupling, enhanced photoluminescence (PL), many-body effects as well as optical nonlinearities.[7]

WS_2 is a prominent representative of the semiconducting TMDC family that has been studied extensively in previous literature. WS_2 consists of two hexagonal sulfur lattices with tungsten atoms occupying trigonal prismatic sites between the sulfur sheets, each WS_2 layer contains a layer of W-atoms with a sixfold coordination symmetry (Figure 6). The hexagonal lattice structure in real space leads to a hexagonal Brillouin zone (BZ) in k-space (Figure 4). The center of the BZ, Γ, is surrounded by the high symmetry points K and M.

For metals of groups IV-VII, each layer is 6-7 Å thick.[8] The bulk material exhibits a layered structure with strong in-plane covalent W-S bonds and weak van-der-Waals (vdW) forces between adjacent layers. Bulk WS_2 exhibits a *2H*-polytype stacking order with a 180° rotation of neighboring layers and belongs to the centrosymmetric D_{6h} point group (*P6₃/mmc* space group).[9] Few-layer WS_2 exhibits different symmetry properties: even layer WS_2 belong to the centrosymmetric D_{3d} point group (*P3m1* space group); odd layer WS_2 belong to the noncentrosymmetric D_{3h} point group (*P6m2* space group). As mentioned, atomically thin layered materials usually exhibit different symmetry properties compared to the corresponding bulk material. Symmetry plays a critical role in the material's properties and might change distinctively even within thickness differences of only one atomic layer. For WS_2, bulk and bi-layer are expected to exhibit inversion symmetry, while single-layer WS_2 is a non-centrosymmetric material, breaking the inversion symmetry.[10,11]

Figure 4 shows the band structure by DFT calculations for bulk and ML (monolayer) WS_2. Bulk TMDCs are indirect band gap semiconductors, with a gap energy of 1.3 eV for bulk WS_2.[9] For bulk WS_2, the splitting of the valence band leads to two prominent indirect transitions (see arrows in Fig. 4b). In the experiment, the laser excites an electron at the Γ-point of the valence band to the K-point of the conduction band, while the difference in momentum (Γ-point *vs.* K-point) is compensated by acoustic phonons. The excited electron interacts by Coulomb-interactions with the empty state in the valence band (the latter called 'hole'), such that a bound electron-hole pair is formed with binding energy of a few 100s of meV. These Coulomb-bound electron-hole pairs are called excitons.[12] After the so-called photoluminescence lifetime, the excitons recombine and send out photons. Photoluminescence (PL) is the light emitted from *e.g.* the WS_2 samples after the absorption of photons from the incoming laser light. In the case of WS_2, there are the two exciton emission lines, namely the so-called *A-exciton* (at an PL-emission energy of 1.94 eV) and *B-exciton*

(2.36 eV). When decreasing the number of layers, the band gap energy increases and a direct band gap forms at the *K*-point in the limit of monolayers due to *d*-orbital interactions and additional quantum confinement effects.[9] The corresponding excitons emit photons at 2.05 eV. The transitions can be measured and evaluated using the advanced lab course setup.
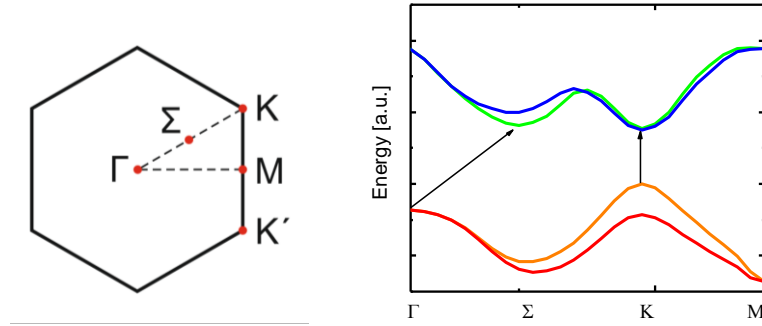

Figure 4: The hexagonal BZ of a TMDC is demonstrated on the left. Band structure of hexagonal WS$_2$ calculated by DFT on the right.

Guideline to proof your understanding of photoluminescence:

6. *What information can you extract from PL measurements of exfoliated WS$_2$ flakes?*
7. *How can you distinguish between the PL of monolayer and bilayer WS$_2$?*

1.3. Second harmonic generation

Non-linear optical properties play an important role in various optoelectronic and photonic applications.

Second harmonic generation (SHG) is a nonlinear optical process (Figure 5). Two photons with the same frequency ω interact with a nonlinear medium and *combine* to generate a photon with double the energy of the initial photons (2ω).[13]
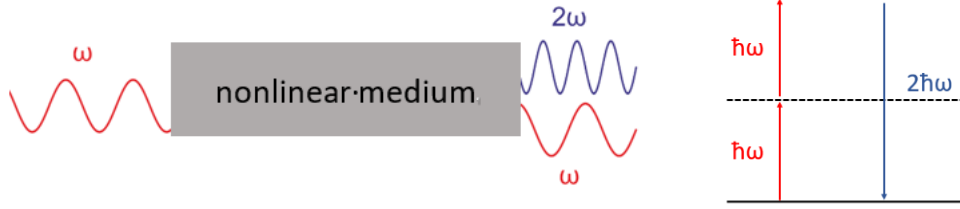

Figure 5: 2nd harmonic generation.
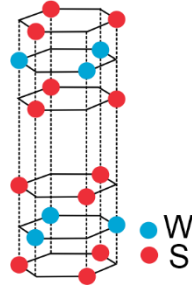
1.3.1.   SHG in WS₂

Figure 6: Repeating structure of two-layer units in 2H-stacked WS₂.

Second order optical nonlinearity $\chi^{(2)}$ in TMDCs is expected due to the lack of inversion symmetry for single-layer and odd number few-layer (FL) TMDCs. The broken inversion symmetry allows valley-selective optical interband transitions. For the D_{3h} symmetry, only the following four elements of the second-order susceptibility tensor are nonzero:[10]

$$\chi_{xxx}^{(2)} = -\chi_{xyy}^{(2)} = -\chi_{yyx}^{(2)} = -\chi_{yxy}^{(2)} = \chi^{(2)}, \tag{3}$$

where *x* corresponds to the armchair direction (as it has a mirror plane symmetry) and *y* is the zigzag direction. Applying the theory of nonlinear SHG, we obtain the following formula that describes the total SHG intensity detected:[10]

$$I_{SHG} = A\left[cos^2(3\theta - 2\varphi)cos^2(\zeta) + sin^2(3\theta - 2\varphi)sin^2(\zeta)\right], \tag{4}$$

A is a multiplication factor depending on the SHG susceptibility tensor $\chi^{(2)}$ and the amplitude of the excitation field. *φ* is the fundamental polarization angle and *θ* is the angle between the *x* crystal axis and

the incidence polarization. We obtain the two normal components of the SHG field when the analyzer orientations are ζ=0 and ζ=π/2:

$$I_X = cos^2(3\theta - 2\varphi) \quad \text{and} \tag{5}$$

$$I_y = sin^2(3\theta - 2\varphi). \tag{6}$$

Furthermore, the electric dipole theory predicts under the first-order perturbation theory that

$$E(2\omega) \propto P^{(2)}(2\omega) = \chi^{(2)}E^2(\omega) \tag{7}$$

$$I_{SHG}(2\omega) \propto |E(2\omega)|^2 \propto \left[\chi^{(2)}E^2(\omega)\right]^2 \propto [I_{funamentals}(\omega)]^2. \tag{8}$$

Hence, the SHG intensity should show a quadratic dependence on the excitation power.

The unusually strong optical SHG is very sensitive to layer thickness, crystalline orientation and layer stacking. Moreover, the finite SHG provides opportunities for new applications in optoelectronic devices such as coherent control of valley-polarized currents.[14]

The setup of the advanced practical training allows to probe the SHG in 2D materials. SHG allows the verification of the broken inversion symmetry of odd layer thicknesses by comparing the SH intensity and further allows to study its evolution with layer thickness.[15,11] For measurements of WS$_2$, it is advisable to limit the average laser power to ~ 3 mW (equivalent to 0 mA current) (*Why is it necessary to limit the power?*). We expect SH intensity of WS$_2$ for odd numbers of layers that decrease significantly with growing layer thicknesses (*e.g.* 1 *vs.* 3 layers). For h-BN (which has a similar structure to WS$_2$ and exhibits the same symmetry properties for odd and even number of layers) the intensity of SH is similar for all odd layers.

Polarization dependence:

Polarization-resolved SHG measurements provide important crystallographic information. Polarized SHG can be used for probing the structural symmetry of 2D materials since the tensor structure of χ$^{(2)}$ is closely related to the material structure symmetry.[10] Polarization-dependent plots are a simple approach for determining the crystallographic direction of *e.g.* WS$_2$. This is especially important for 2D heterostructures or nanoribbons, as their physical properties depend on the relative 2D crystal stacking orientation.[16] As mentioned above, the polarized SH signal is proportional to *Θ*. The relationship can be shown in a polar plot and can be compared to experimental data. The symmetry of the atomic structure predicts the polarized SH intensity to be maximized for excitation along the armchair direction and zero along the zigzag direction (as shown in Figure 7).
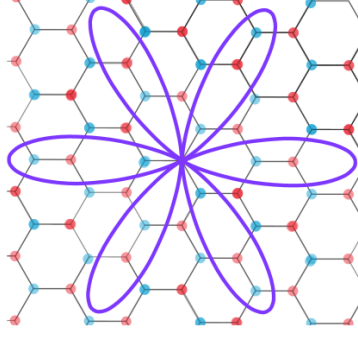
Figure 7: Sketch of the polarization-resolved SHG intensity in connection with the underlying crystal geometry.

Guideline to proof your understanding of polarization dependent SHG:

8. *What geometry do you expect for the polar plot showing normalized polarization dependence of SHG in WS$_2$?*

The weak dielectric screening in atomically thin materials enhances the Coulomb interaction between electrons and holes. Hence, the matrix elements of optical transitions are greatly enhanced. Consequently, the nonlinear susceptibility of TMDs has an absolute value of a few nm/V, which is orders of magnitude larger than that for common nonlinear crystals.[11] Exciting a TMDC monolayer with linear polarized light under normal incidence and subsequent filtering of the SHG response with a linear polarizer, oriented along the fundamental polarization angle, results in a six-fold SHG intensity pattern.

Literature has shown that mechanical strain can reduce the symmetry of a crystal and therefore change the nonlinear susceptibility. The six-fold SHG symmetry is often broken even without externally applied strain and can be attributed to the exfoliation and transfer process (uniaxial strain).[10]

The strain can be modeled using a second-order nonlinear photoelastic tensor which translates the strain tensor u_{lm} linearly into a contribution to the nonlinear susceptibility tensor of the unstrained crystal $\chi_{ijk}^{(2,0)}$. The total nonlinear susceptibility is then given as:

$$X_{ijk}^{(2)} = X_{ijk}^{(2,0)} + p_{ijklm}u_{lm} \tag{9}$$

Under these conditions, 12 nonzero elements occur.[10]

The strain angle θ, is given relative to the *x*-axis and thus independent of the crystal orientation.

By calculating the parallel polarization-resolved SHG response, the strain dependent SHG intensity at the polarization direction φ is described as[10]

$$I_\parallel^{(2)}(2\omega) \propto (A cos(3\varphi - 3\delta) + B cos(2\theta + \varphi - 3\delta))^2. \tag{10}$$

10

The first term with pre-factor A depends on the sum of the two strain elements ε_{xx} and ε_{yy} and directly changes the nonlinear susceptibility tensor element of the unstrained crystal $X_0^{(2)}$. The second term with the pre-factor B depends on the difference of the principal strain components ε_{xx} and ε_{yy}. The B term vanishes if the crystal strain is purely biaxial ($\varepsilon_{xx} = \varepsilon_{yy}$). The B term of the equation becomes nonzero only if the symmetry is broken by strain, resulting in a symmetry-breaking of the SHG intensity pattern along the principal strain tensor angle θ. The symmetry breaking depends on the sample orientation which can be verified by rotating the samples by 90°.
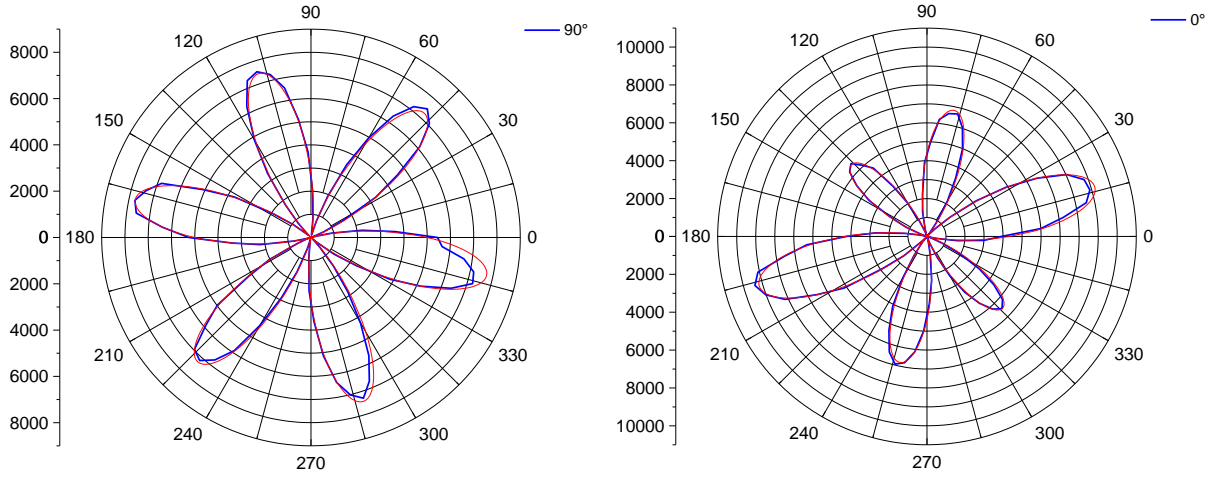

Figure 8: Polarization-resolved SHG intensity of WS2 with cross (90°)- and co(0°)-polarization. Both show the expected 6-fold symmetry. All petals distribute similar intensities for 90°, but vary for 0°.

2. Experiment

2.1. Raman and photoluminescence setup

Figure 9: The experimental setup for the advanced practical training (WITec, alpha 300 R).

For the Raman and PL measurements, a green laser (532 nm) is focused on the sample surface. In general, the Raman scattering is larger for shorter wavelengths due to the v^2 increase in the Raman scattering cross-section.[17] To separate the Raman from the Rayleigh scattered light, a notch or long-pass optical filter is implemented in the optical path.

Guideline to proof your understanding of the experimental setup:

9. *Make yourself familiar with the confocal Raman microscopic setup. Make a simplified sketch of the Raman setup for your report.*
10. *What are the disadvantages of using shorter wavelength lasers in an optical path?*

2.2. SHG setup
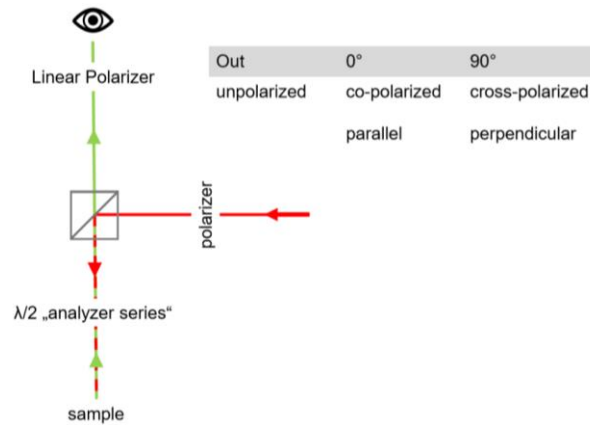
Figure 10: Schematic of the WITec setup for SHG measurements.

For the SHG measurements we use a 1064 nm laser with 0 mA drive current (= 3 mW) which is directed to a confocal scanning laser microscope modified for two photon excitation. The laser is focused on the sample at normal incidence by a 100x objective (NA 0.9). The back reflected signal is directed to the dichroic mirror. A narrow bandpass filter is centered at the SH wavelength to completely remove the laser scattered light. The laser is focused onto the sample at normal incidence with a fixed linear polarization that is in the plane of the sample.

3. Experimental procedure

3.1. Safety instructions

It is essential that you understand the following safety measures:

- ➢ Do **NOT** stare into the laser light! These are class 3B lasers. Direct eye contact with the output beam from a 3B laser will cause serious damage and possibly blindness. **Always** put the magnetic cover in front of the sample to protect yourselves and especially others passing the setup from laser harm.
- ➢ Do not touch anything in the lab beside the experimental setup and only touch the setup after you have been given an introduction by your advisor.
- ➢ Do not eat or drink in the lab.
- ➢ In case of a fire alarm, leave the room immediately. Gather at the meeting point next to the northern *Physik II* entrance.

3.2. Exfoliation of graphite and WS_2

Note down temperature and humidity, as well as time and day of measurement.

You have been provided with a scotch tape full of bulk crystals of graphite/WS_2 distributed on the tape.

1. Prepare the glass slide and make sure it's clean ➔ remove fingerprints, dust *etc.* with IPA (Isopropanol; yellow bottle) and paper towels (wear gloves to keep glass slide free of fingerprints).
    a. For **graphite**, you may exfoliate directly onto the glass slide, proceed to step 2.
    b. For **TMDCs**, exfoliate onto a Si/SiO_2 wafer. For this, use a double-sided tape to place the wafer onto a clean glass slide and proceed with step 2.
2. Separate tapes (carefully with tweezers) and make sure to keep the tapes clean. Put one half of the tape aside.
3. Use the other half of the tape to transfer material onto the glass slide/wafer. Put the sticky side of the tape onto the glass slide/wafer (maybe apply a little pressure onto the tape).
4. Remove tape slowly leaving residual flakes on the glass slide/wafer.

3.3. Raman measurements on graphite

Follow the manual for the WITec setup step by step and put your name, date and measurement info into the logbook.

Turn on the imaging mode and extract an overview image of your sample (stitching *via* the four squares icon). Make yourself familiar with your sample, take a close look at it and evaluate which flakes (choose 3) you want to measure. For choosing the optimal flakes, take following points into account:

> ➢ One of the three flakes should be as thin as possible and if possible *undefected.*
>
> ➢ One of the three flakes should be thicker but still few layer.
>
> ➢ One of the three flakes should have cracks and tears.

Acquire one spectrum of each flake (3 spectra in total). Analyze the spectra to obtain parameters such as the resonance intensities, positions and FWHM. Extract following information for the report:

> I. *How does the Raman signal depend on the layer thickness?*
> II. *How do cracks/defects influence the Raman spectrum?*
> III. *How does a substrate, including yours, influence the Raman signals?*

3.4. Raman and PL measurements on WS_2

Turn on the imaging mode and extract an overview image of your sample (stitching *via* the four squares icon). Make yourself familiar with your sample, take a close look at it and evaluate which flakes you want to measure. You will measure a photoluminescence (PL) map of an area of ~10 x 10 µm. For choosing the optimal flakes, take following points into account:

> ➢ Generally, the PL signal is strongest for ML WS_2. For our purposes, we want to evaluate how the PL signal evolves with layer thickness. Hence, search for a flake with different layers (or thicker and thinner flakes in close vicinity).

Move the grating to the correct energy values. Acquire a PL map. For this, choose *Large area scan*, choose region of interest with *Listen position* and enter number of measurements with *Points per Line* and *Lines per Image.* Set the integration time and accumulations, then *Start Large Area Scan.* Analyze the spectra to obtain parameters such as the resonance intensities, positions and FWHM. Extract following information for the report:

IV. *Roughly which PL intensities do you expect? Explain the PL signal you obtained theoretically.*

V. *Calculate the excitonic binding energy using the determined resonance energy from your measurements.*

3.5. SHG measurements on WS_2

Carefully read the measurement manual for the WITec setup (SHG chapter).

Choose a WS_2 flake with at least three different thicknesses (if you have already done so for the PL map, you may use the same flake if at least one layer shows SHG signal).

Measure an SHG map. Choose a spot with the highest SHG signal from the SHG map and start a polarization dependent measurement. For this, put the analyzer into the beam path at 0° (hardware) and start an analyzer series (*Series slow → analyzer series*). Choose the measurement points. Plot the obtained spectra as a polar plot. Extract following information for the report:

VI. *What does the SHG signal depend on?*

VII. *For which samples/layers can we expect an adequate SHG signal?*

VIII. *What do the signals of your measurements tell you about the layers?*

IX. *What do you expect for the polar plot and why? How can you explain possible deviations?*

4. Writing the report

Use *WITec Project* to process and analyze your data. Think about what needs to be done (background subtraction, smoothing, peak analysis *etc.*)

Either plot the data with *WITec Project* or use a familiar application such as *origin* or *mathematica*, which are installed on PCs in CIP pool. The plots should be consistent and entail all important information including axes descriptions and units.

Not all questions given in the experimental procedure chapter must be answered. This is just an orientation of what might be important. Each sample, parameters, conditions *etc.* are different, so concentrate on your sample and utilize literature – WS_2 and graphene are both very popular and well-studied materials, there's plenty of literature you can rely on (see Appendix).

Please keep the following scientific standards in mind:

➢ The report should have a clear structure with a *red thread.*

➢ The report should include an introduction (physical background), experimental setup, experimental parameters and implementation. The focus should be set on the results and discussion and the report should be rounded up with a quick summary.

➢ Include references and give proper citations.

➢ Graphs should always be labelled on each axis and discussed in detail. Compare your results to literature and argue differences/similarities.

➢ A spectrum/measurement is useless if the reader can't reproduce/comprehend your measurement. Therefore, all important parameters must be added (*e.g.* as a table or list).

➢ Quality over quantity → re-read your report and keep your phrasing short and on point. This is good practice for future theses.

4.1. Raman measurements on graphite

This part should contain:

a) An image of the measured flakes that are assigned to each spectrum (This you can do in the WITec project application by dragging the spectrum into the video stitch image).

b) All evaluated spectra, including a table with the parameters such as position, FWHM, …

c) Add the conical plots for each peak you evaluate (similar to *question 2*).

d) Answers to the questions *I-III*.

4.2. Raman and PL measurements on WS_2

This part should contain:

a) An image of the measured flakes that are assigned to each measurement.

b) All evaluated spectra, including a table with the parameters

c) PL map and the theoretical explanation behind the PL signal of WS_2

d) Answers to the questions *IV-VI*

4.3. SHG on WS_2

This part should contain:

a) An image of the measured flakes that are assigned to each measurement.

b) The SHG map.

c) Polar plot(s) of an SHG-intense position.

d) Answers to the questions *VII-X.*

5.   Appendix

Additional information can be found in the following publications, on which this manuscript is based on:

Raman

Raman spectroscopy in graphene, *Malard et al.*, 2009

Raman spectroscopy as a versatile tool for studying the properties of graphene, *Ferrari et al.*, 2013

Raman spectroscopic characterization of graphene, *Bo et al.*, 2010

Spatially resolved Raman spectroscopy of single- and few-layer graphene, *Graf et al.*, 2007

PL

Distinct photoluminescence and Raman spectroscopy signatures for identifying highly crystalline WS_2 monolayers produced by different growth methods, *McCreary et al.*, 2016

SHG

Probing Symmetry Properties of Few-Layer MoS_2 and h-BN by Optical Second-Harmonic Generation, *Li et al.,* 2013

Extraordinary Second Harmonic Generation in Tungsten Disulfide Monolayers, *Janisch et al.*, 2014

Second harmonic generation in strained transition metal dichalcogenide monolayers: MoS_2, $MoSe_2$, WS_2, and WSe_2, *Mennel et al.*, 2018

6. References

1. Casiraghi, C., Pisana, S., Novoselov, K. S., Geim, A. K. & Ferrari, A. C. Raman fingerprint of charged impurities in graphene. *Appl. Phys. Lett.* **91**, 2007–2009 (2007).

2. Ni, Z. H. *et al.* Raman spectroscopy of epitaxial graphene on a SiC substrate. *Phys. Rev. B - Condens. Matter Mater. Phys.* **77**, 1–20 (2008).

3. Bayle, M. *et al.* Determining the number of layers in few-layer graphene by combining Raman spectroscopy and optical contrast. *J. Raman Spectrosc.* 36–45 (2018) doi:10.1002/jrs.5279.

4. Franken, P. A., Hill, A. E., Peters, C. W. & Weinreich, G. Generation of optical harmonics. *Phys. Rev. Lett.* **7**, 118–119 (1961).

5. Malard, L. M., Pimenta, M. A., Dresselhaus, G. & Dresselhaus, M. S. Raman spectroscopy in graphene. *Phys. Rep.* **473**, 51–87 (2009).

6. Ferrari, A. C. & Basko, D. M. Raman spectroscopy as a versatile tool for studying the properties of graphene. *Nat. Nanotechnol.* **8**, 235–246 (2013).

7. Wurstbauer, U., Miller, B., Parzinger, E. & Holleitner, A. W. Light-matter interaction in transition metal dichalcogenides and their heterostructures. *J. Phys. D. Appl. Phys.* **50**, (2017).

8. Wu, R. J., Odlyzko, M. L. & Mkhoyan, K. A. Determining the thickness of atomically thin MoS2 and WS2 in the TEM. *Ultramicroscopy* **147**, 8–20 (2014).

9. Liu, G. Bin, Xiao, D., Yao, Y., Xu, X. & Yao, W. Electronic structures and theoretical modelling of two-dimensional group-VIB transition metal dichalcogenides. *Chem. Soc. Rev.* **44**, 2643–2663 (2015).

10. Mennel, L., Paur, M. & Mueller, T. Second harmonic generation in strained transition metal dichalcogenide monolayers: MoS 2 , MoSe 2 , WS 2 , and WSe 2. *APL Photonics* **4**, (2019).

11. Janisch, C. *et al.* Extraordinary second harmonic generation in Tungsten disulfide monolayers. *Sci. Rep.* **4**, 1–5 (2014).

12. Gutierrez, H. R. *et al.* Extraordinary room-temperature photoluminescence in WS2 triangular monolayers. *Nano Lett.* **13**, 3447–3454 (2012).

13. Zhou, X. *et al.* Strong Second-Harmonic Generation in Atomic Layered GaSe. *J. Am. Chem. Soc.* **137**, 7994–7997 (2015).

14.   Kiemle, J., Zimmermann, P., Holleitner, A. & Kastl, C. Light-field and spin-orbit-driven currents in van der Waals materials. *Nanophotonics* **9**, (2020).

15.   Li, Y. *et al.* Probing symmetry properties of few-layer MoS2 and h-BN by optical second-harmonic generation. *Nano Lett.* **13**, 3329–3333 (2013).

16.   Hsu, W. T. *et al.* Second harmonic generation from artificially stacked transition metal dichalcogenide twisted bilayers. *ACS Nano* **8**, 2951–2958 (2014).

17.   Bischel, W. K. & Black, G. Wavelength dependence of raman scattering cross sections from 200-600 nm. *AIP Conf. Proc.* **100**, 181 (1983).